Chemical Science

ROYAL SOCIETY OF CHEMISTRY

EDGE ARTICLE

View Article Online
View Journal | View Issue

Cite this: *Chem. Sci.*, 2020, **11**, 12477

All publication charges for this article have been paid for by the Royal Society of Chemistry

Received 4th September 2020
Accepted 20th October 2020

DOI: 10.1039/d0sc04886k

rsc.li/chemical-science

The sporothriolides. A new biosynthetic family of fungal secondary metabolites†

Dong-Song Tian, [a] Eric Kuhnert, [a] Jamal Ouazzani, [b] Daniel Wibberg, [c] Jörn Kalinowski [c] and Russell J. Cox *[a]

The biosynthetic gene cluster of the antifungal metabolite sporothriolide **1** was identified from three producing ascomycetes: *Hypomontagnella monticulosa* MUCL 54604, *H. spongiphila* CLL 205 and *H. submonticulosa* DAOMC 242471. A transformation protocol was established, and genes encoding a fatty acid synthase subunit and a citrate synthase were simultaneously knocked out which led to loss of sporothriolide and sporochartine production. *In vitro* reactions showed that the sporochartines are derived from non-enzymatic Diels–Alder cycloaddition of **1** and trienylfuranol A **7** during the fermentation and extraction process. Heterologous expression of the *spo* genes in *Aspergillus oryzae* then led to the production of intermediates and shunts and delineation of a new fungal biosynthetic pathway originating in fatty acid biosynthesis. Finally, a hydrolase was revealed by *in vitro* studies likely contributing towards self-resistance of the producer organism.

Gamma-lactone and alkyl citrate compounds derived from oxaloacetate are widespread natural products in fungi and often possess potent biological activities. Examples include sporothriolide **1**,[1,2] piliformic acid **2**,[3] tyromycin **3**[4] and the cyclic maleidrides including byssochlamic acid **4**[5,6] among others (Fig. 1). In some cases, for example those of **4** and squalestatin S1 **5**,[7] detailed molecular studies have revealed that a dedicated polyketide synthase (PKS) produces a carbon skeleton that is then condensed with oxaloacetate by a citrate synthase (CS) to give an early alkyl citrate intermediate that is further oxidatively processed. In other cases, such as **1** and the sporochartines **6**, the biosynthetic pathways are not yet clear.

Sporochartines **6a–6d**[8,9] from the fungus *Hypoxylon monticulosum* CLL 205 (now referred to as *Hypomontagnella spongiphila*)[10] possesses potent cytotoxicity (IC_{50}: 7.2 to 21.5 μM) *vs.* human cancer cell lines and are proposed to be Diels Alder (DA) adducts of the furofurandione sporothriolide **1**, itself a potent antifungal agent (EC_{50}: 11.6 ± 0.8 μM),[11] and trienylfuranol A **7**,[12] originally obtained from an endophytic fungus *Hypoxylon submonticulosum* DAOMC 242471 (now referred to as *Hypomontagnella submonticulosa*).[13] Since the biosynthesis of sporothriolide **1** and related compounds is unknown, and biological DA reactions in fungi are currently of high interest,[14] we decided to examine the biosynthesis of the sporochartines **6** in the *Hypomontagnella* spp. strains MUCL 54604 and CLL 205 (ref. 10 and 13) in detail.

Results

The three known producers of sporochartines, sporothriolide **1** and trienylfuranol A **7** (*H. monticulosa* MUCL 54604, *H. spongiphila* CLL-205 and *H. submonticulosa* DAOMC 242471) were grown in PDB liquid media and examined for production of

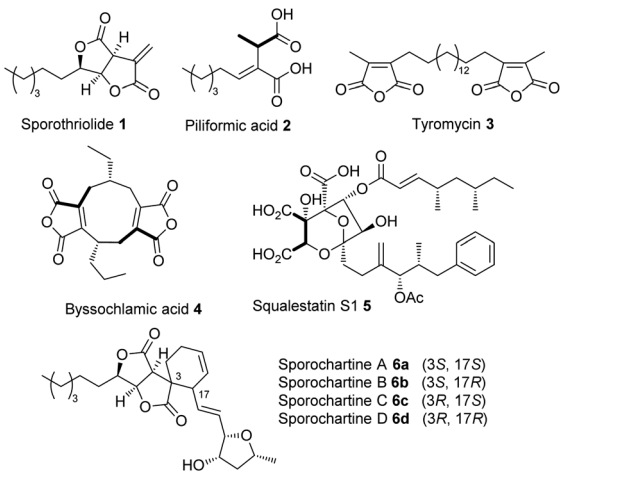

Fig. 1 Structures of γ-lactone and alkyl citrate metabolites from fungi. Bold bonds show oxaloacetate-derived carbons where known.

[a]*Centre of Biomolecular Drug Research (BMWZ), Institute for Organic Chemistry, Leibniz University Hannover, Schneiderberg 38, 30167, Hannover, Germany. E-mail: russell.cox@oci.uni-hannover.de*

[b]*French National Center for Scientific Research (CNRS), Institute for the Chemistry of Natural Substances (ICSN), Avenue de la Terrasse, 91198, Gif-sur-Yvette, Cedex, France*

[c]*Center for Biotechnology (CeBiTec), Bielefeld University, Universitätsstraße 27, 33615, Bielefeld, Germany*

† Electronic supplementary information (ESI) available: including all experimental and spectroscopic details. See DOI: 10.1039/d0sc04886k

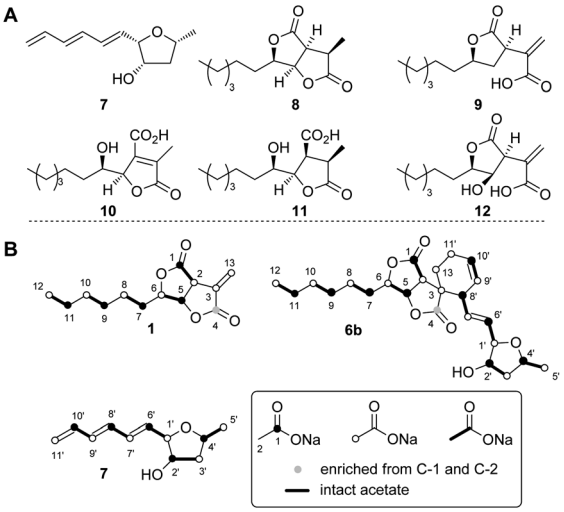

Fig. 2 (A) Isolated compounds from *H. spongiphila* CLL 205. (B) Isotope labelled compounds from [1-^{13}C], [2-^{13}C] and [1,2-^{13}C$_2$]-acetate feeding experiments.

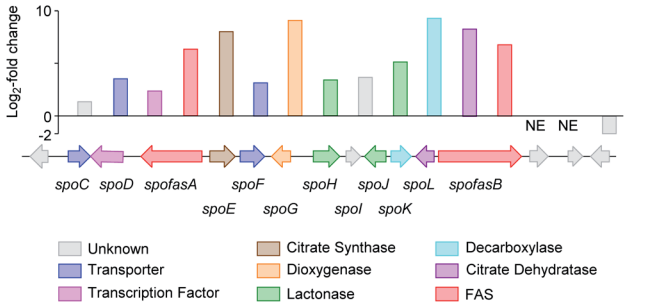

Fig. 3 Transcriptome analysis of the sporothriolide BGC from *H. monticulosa* MUCL 54604. Log 2-fold changes are calculated between producing and non-producing conditions. NE, no expression.

metabolites by LCMS. Production time course experiments (see ESI Fig. S1.11–S1.14†) showed a high production of sporothriolide **1** in all three organisms (*ca* 180–238 mg L^{-1}), as well as very low titers of sporochartine B **6b** (*ca* 4–6 mg L^{-1}). Compounds **1**, **6b** and **7**, and cometabolites **8–12** (Fig. 2) were purified, characterised by 1D NMR and compared to literature (see ESI Tables S3.1–S3.8†). All three fungi are also capable of producing trienylfuranol A **7**, but the *H. submonticulosa* strain yields higher amounts.

The biosynthetic origin of the different carbon chains in **1**, **6b** and **7**, was determined by isotopic labelling experiments with [1-^{13}C], [2-^{13}C] and [1,2-^{13}C$_2$] acetate (see ESI Tables S1.11–S1.13†). The observed labelling patterns of compounds **1** and **6b** were consistent with a fatty acid or polyketide origin (see ESI Table S1.2†), coupled to a decarboxylated Krebs cycle intermediate such as oxaloacetate (Fig. 2). Carbons C-6 and C-1′ of **6b** derived from C-2 of acetate were oxygenated indicating the involvement of an oxygenase during biosynthesis. Trienylfuranol A **7** was also shown to be derived from at least six intact acetates, but the loss of a C-1 acetate-derived carbon at C-11′, and oxygenation at C-1′ once again suggests the involvement of oxidative steps.

Genomic DNA from all three organisms was sequenced and assembled to afford high quality draft genomes (see ESI Table S1.1†).[10] antiSMASH[15] fungal version predicted 72, 69 and 53 secondary metabolite biosynthetic gene clusters (BGC) in the CLL, MUCL and DAOMC genomes, respectively (see ESI Fig. S1.1†).

Initial searches for BGC containing PKS and CS encoding genes, as found for the biosynthesis of related compounds such as **4** and **5**, were not productive. However, search for fungal fatty acid synthase (FAS) genes co-located with CS genes, as found for example in the BGC for the oryzines,[16] rapidly identified closely related target BGC in all three organisms, which also encoded the expected oxygenase and decarboxylase catalysts (Fig. 3). BLASTp[17] and PHYRE2 (ref. 18) platforms were used to annotate and predict the putative function of all proteins encoded by the BGC (see ESI Table S1.2†). In addition to the expected citrate synthase *spoE*, and two fungal FAS subunits (FASα and FASβ) *spofasA* and *spofasB*, the BGC was found to encode: a methylcitrate dehydratase (*spoL*); a decarboxylase (*spoK*) similar to the *cis*-aconitate decarboxylase;[19] a dioxygenase (*spoG*); and two putative lactonases (*spoH* and *spoJ*). In addition, the clusters encoded two transporters (*spoC* and *spoF*), along with a transcriptional regulator (*spoD*), and *spoI* with unknown function (GenBank MT889334, see ESI Table S1.3†). The three clusters were highly homologous, containing the same genes in the same order and orientations (see ESI Fig. S1.3 and S1.4†).

RNA from *H. monticulosa* MUCL 54604 was isolated separately under **1** and **6b** producing (PDB medium) and non-producing (DPY medium) conditions and subjected to transcriptome sequencing (see ESI S1.1.3 for details†). Differential gene expression analysis of the predicted functional genes from *spofasB* to *spofasA*, showed a strong upregulation under producing condition (Fig. 3), while genes outside this region showed either low expression (see ESI Table S1.4†) or no change in transcription level.

The *spoE* (CS) and *spofasA* genes in *H. spongiphila* CLL 205 were then deleted simultaneously. This was achieved using the bipartite method of Nielsen and coworkers[20] to insert a hygromycin resistance cassette. Forty-six hygromycin resistant transformants were generated and cultivated under sporothriolide **1** producing conditions and compared to the wild type (WT) strain (Fig. 4). One of these produced neither sporothriolide **1** nor the related sporochartines **6** or congeners **8–12**. Polymerase chain reaction (PCR) analysis confirmed the incorporation of the hygromycin resistance gene at the target position and successful disruption of *spoE* and *spofasA* (see ESI Fig. S1.9 and S1.10†).

In this mutant the titre of trienylfuranol A **7** was increased, and this strain was therefore a suitable organism for the purification of **7** in usable amounts (*e.g.* 40 mg L^{-1}). Sporochartines are formed as mixtures of diastereomers at the cyclohexene moiety and the observation that the *endo* DA product **6b** always occurs in higher amounts than *exo* adduct **6a** can be explained by the preference of DA reactions for *endo* product formation

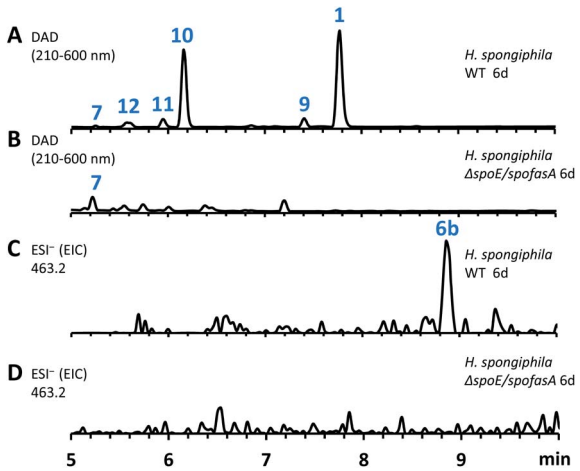

Fig. 4 HPLC analysis of crude extracts from *H. spongiphila* CLL 205 grown under producing conditions of **1**: (A), Diode Array Detector (DAD) chromatogram of wild-type (WT); (B), DAD chromatogram of Δ*spoE*/*spofasA*; (C), extracted ion chromatogram (EIC of **6b**, ESI⁻, 463.2, M + HCOO⁻) of WT extract; (D), EIC of Δ*spoE*/*spofasA* transformant showing absence of **6b**.

over *exo*. We therefore considered it possible that the proposed DA condensation between sporothriolide **1** and trienylfuranol A **7** could be non-enzymatic. In order to probe this question, we first added sporothriolide **1** to the supernatant obtained from the *H. spongiphila* Δ*spoE*/*spofasA* strain grown under producing conditions of **1** to accumulate **7**. After 24 h of incubation **6a**/**6b** were observed in the medium by HPLC-MS (Fig. 5B). In

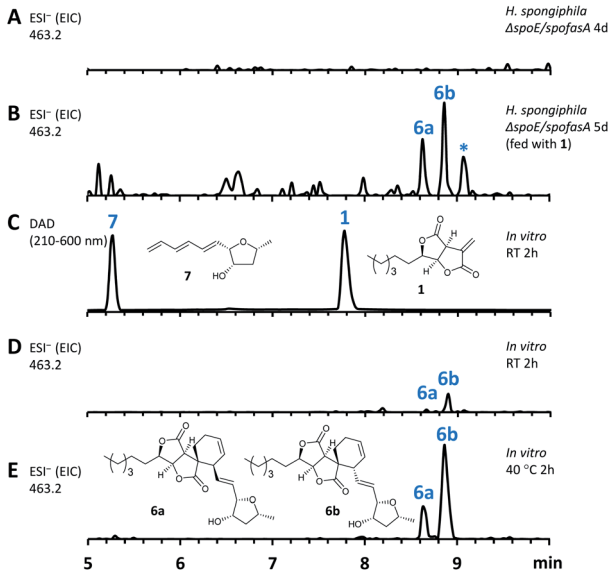

Fig. 5 *In vivo* and *in vitro* assay for spontaneous sporochartine (**6a** and **6b**) production. (A) Extracted ion chromatogram (EIC of **6a**/**6b**, ESI⁻, 463.2, M + HCOO⁻) of crude extract from *H. spongiphila* CLL 205 Δ*spoE*/*spofasA*; (B), EIC of **6a**/**6b** from *H. spongiphila* CLL 205 Δ*spoE*/*spofasA* fed with **1**; (C) and (D) UV/vis spectrum and EIC (**6a**/**6b**) of *in vitro* reaction between **7** and **1** in ethyl acetate at RT, 2 h; (E), EIC (**6a**/**6b**) of *in vitro* reaction between **1** and **7** in ethyl acetate at 40 °C, 2 h. *Unrelated peak.

addition, **1** and trienylfuranol A **7** were also reacted under nitrogen in the dark in ethyl acetate (the standard extraction solvent). After 2 hours at room temperature, sporochartine A **6a** (minor) and sporochartine B **6b** (major) were observed by LCMS (Fig. 5D). At 40 °C (Fig. 5E), the reaction accelerated to give the same compounds in higher titre (see ESI S1.2.11 for details†).

Further analysis of the biosynthesis was performed by heterologous expression of combinations of the *spo* genes in *Aspergillus oryzae* NSAR1 (Table 1 and Fig. 6). All gene fragments were amplified from cDNA and cloned into fungal expression vectors (see ESI Fig. S1.8†). Expression of the FAS components alone, or with addition of the CS (*spoE*) and DH (*spoL*) did not result in the production of new compounds observable by LCMS (Table 1, entries 1–3).

However, heterologous expression of all eight genes (Table 1, entry 8) led to the observation of a range of new metabolites in *A. oryzae* including sporothiolide **1** after 4 days (Fig. 6E). After longer fermentation up to 7 days these were converted to **13** (*ca* 8 mg L^{-1}, Fig. 6G) which has the same molecular formula as sporothriolide ($C_{13}H_{18}O_4$), but a slightly different retention time. Isolation and full NMR analysis of **13** showed this to be the monocyclic analog of **1**, named dehydro-deoxysporothric acid, presumably either resulting from an eliminative ring opening of **1** itself, or being a biosynthetic precursor. However experiments with sporothriolide **1** itself showed that this compound is converted to the observed **13** after exposure to PDB, DPY or CMP fermentation media (pH 5.6–6.5) for short periods (see ESI Fig. S1.19†).

Further experiments were then conducted using reduced *spo* gene sets (Table 1, EXP 4–7). The results of EXP4 then indicated a biosynthetic pathway in which the fungal FAS proteins produce a dedicated decanoic acid **17**, probably as a CoA thiolester, as these proteins possess a bifunctional malonyl-palmitoyl transferase (MPT) domain which loads malonyl CoA and off-loads an acyl CoA.[21] Decanoyl CoA **17** is likely to be reacted with oxaloacetate by CS, in analogy to other known pathways,[6] to give an octanyl citrate **18** which is then dehydrated to give octanyl aconitate **19** and decarboxylated to the first observable intermediate, octanyl itaconic acid **20**, a known compound from the endophytic fungus *Pestalotiopsis theae*.[22] The *R* absolute configuration at C-2 was confirmed by comparing the optical rotation with literature (see ESI Table S3.12†).[22]

The addition of the putative dioxygenase *spoG* to the previous set of genes in *A. oryzae* results in formation of a broad range of new compounds in addition to **20** (EXP 5, Fig. 6B). Four of the observed products (**9**, **12**, **15**, **23**) were purified and their structures were deduced by NMR (see ESI Tables S3.5–S3.11†). Compound **23** was identified as the C-5 hydroxylated product of **20**, which quickly converts in solution into the ring-closed shunt **16** (see ESI Fig. S3.59†). Compound **12** was shown to be sporothric acid, characterized by a lactone ring established between C-6 and the carboxylic acid group of the fatty acid chain.

Due to the presence of a hydroxyl group at C-5, we assume that **12** is derived from a double hydroxylated intermediate **22**, which undergoes spontaneous lactonization and thus putatively

Table 1 Combinations of *spo* genes expressed in *A.oryzae* NSAR1

	spo								
	fasA	*E*	*G*	*H*	*J*	*K*	*L*	*fasB*	
EXP	FASA	CS	DO	Lact	Lact	DC	DH	FASB	Products
1	✓	—	—	—	—	—	—	✓	—
2	✓	✓	—	—	—	—	—	✓	—
3	✓	✓	—	—	—	—	✓	✓	—
4	✓	✓	—	—	—	✓	✓	✓	**20**
5	✓	✓	✓	—	—	✓	✓	✓	**9, 12, 14–15, 20, 22–23**
6	✓	✓	✓	✓	—	✓	✓	✓	**9, 12, 20, 22–23**
7	✓	✓	✓	—	✓	✓	✓	✓	**9, 12, 20, 22–23**
8	✓	✓	✓	✓	✓	✓	✓	✓	**1, 9, 13–15**

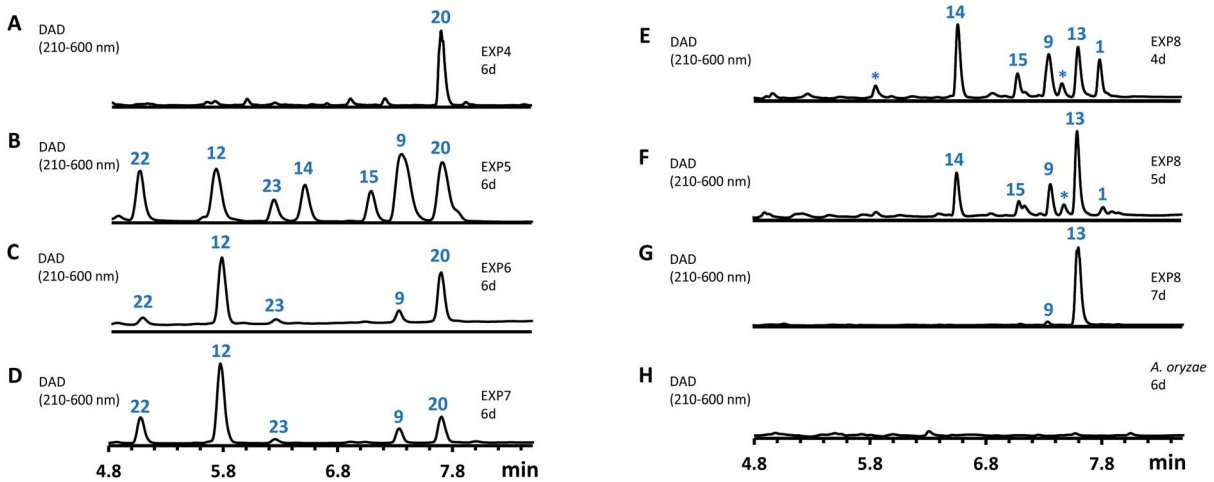

Fig. 6 HPLC analysis of the expression of *spo* genes in *A. oryzae*. (A–H), diode array detector (DAD) traces of extracts of *A. oryzae* transformants. EXP refers to the gene combinations in Table 1.

represents a pathway intermediate. A main peak corresponding with the molecular formula for **22** was observed in the crude extract, but could not be purified to support its identity as the proposed intermediate. Compound **9** is structurally related to **12**, but lacks the hydroxyl group at C-4. It is most likely a shunt metabolite derived from the putative monohydroxylated intermediate **21**. Compound **15** is also monohydroxylated at C-6, but instead of the lactone ring it contains a maleic anhydride. Likewise **15** is probably also derived from the putative intermediate **21** through spontaneous reaction of the carboxylic acid moieties. Isolation of **14** was not successful, and LCMS chromatograms showed that **14** was partially converted to **10** in a short time (see ESI Fig. S3.46–S3.48†). As **14** shares the same molecular formula and very similar retention time with **10** its structure was deduced as the isomeric form of **10**, which itself is likely formed by spontaneous lactonization between C-5 and the carboxylic acid moiety derived from oxaloacetate of the putative intermediate **22**.

As neither the presence of **21** nor **22** could be unambiguously proved in the extracts of the *A. oryzae* transformants due to their instability or quick conversion, the function of SpoG was further evaluated *in vitro*. The *spoG* gene was amplified from *H. monticulosa* MUCL 54604 cDNA and cloned into pET28a (Novagen), then transformed and expressed into *Escherichia coli* BL21.[23] SpoG was purified by fast protein liquid

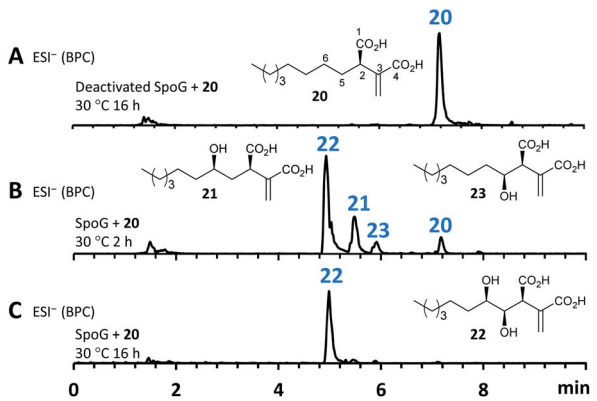

Fig. 7 *In vitro* assay of SpoG using purified proteins. (A), ESI⁻ trace of boiled SpoG (50 μm) incubated with **20** (2.5 mM), Tris buffer (50 mM, pH 7.5), ascorbate (4 mM), α-ketoglutarate (4 mM), and $FeSO_4$ (0.2 mM) at 30 °C, 16 h; (B), ESI⁻ trace of SpoG incubated with **20** under the same conditions for 2 h; (C), ESI⁻ trace of SpoG incubated with **20** under the same conditions for 16 h.

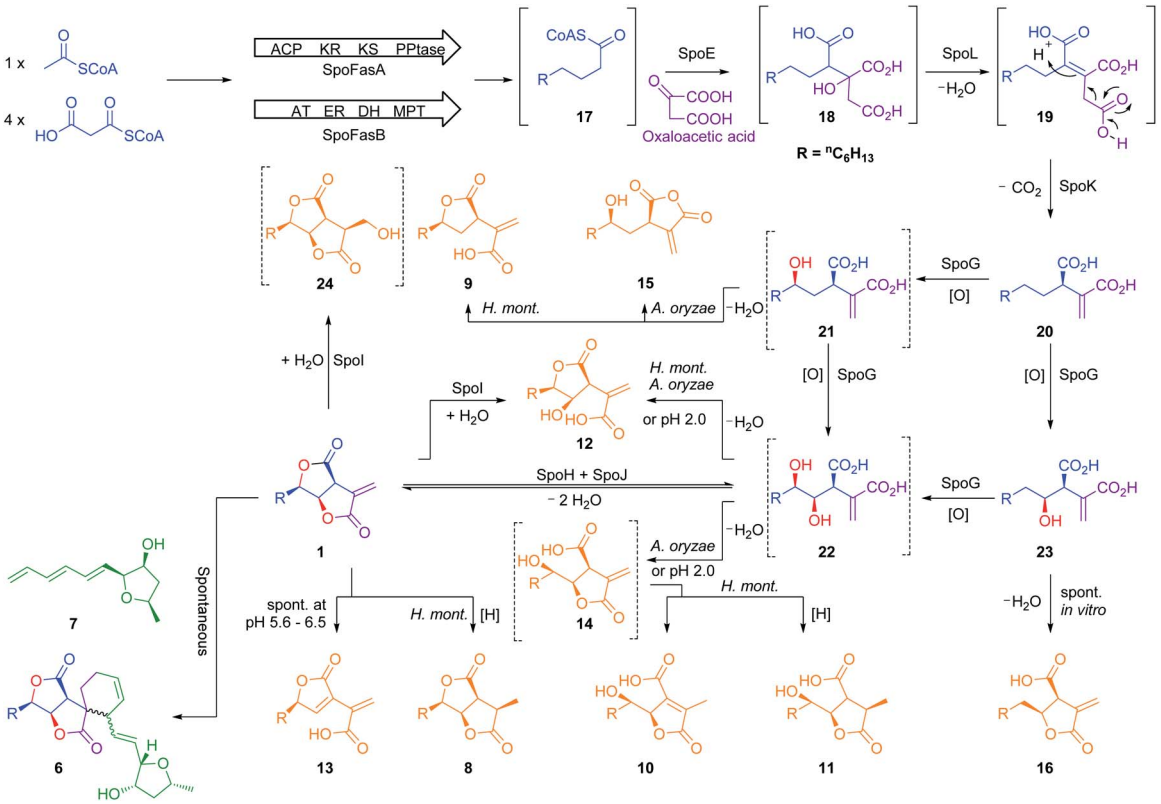

Scheme 1 Proposed biosynthesis of sporothriolide **1** and sporochartines **6**. Orange compounds result from shunt steps. Compounds in solid square brackets were not experimentally observed and those in dashed brackets were observed during experiments but structures could not be confirmed by NMR. Abbreviations: AT, acyl transferase; ER, enoyl reductase; MPT, malonyl palmitoyl transferase; ACP, acyl carrier protein; KR, ketoreductase; KS, ketosynthase; PPTase, phosphopantetheinyl transferase.

chromatography (FPLC) as a soluble protein (see ESI Fig. S1.20–S1.22†). Sequence analysis indicated that SpoG requires α-ketoglutarate as a cofactor. Incubation of purified SpoG with intermediate **20**, $FeSO_4$, α-ketoglutarate, and ascorbate at 30 °C for 2 h led to the formation of three products, the main compound of which was identical with **22** (by mass, UV and retention time) from the heterologous expression experiments. In addition, **23** was formed as minor product alongside another compound with identical mass likely representing its proposed regioisomer **21** (Fig. 7B). Extended incubation times up to 16 h resulted in a complete conversion of **21** and **23** into **22** indicating that **21** and **23** are precursors of **22** and that SpoG catalyses two consecutive rounds of hydroxylation (Fig. 7C). These results show that SpoG catalyses hydroxylation at C-5 and C-6 of the saturated carbon chain, and that the pathway is conducted *via* **21** and **23**.[24]

The presence of **21** and the lack of its putative shunts **15** and **9** in the *in vitro* setup indicates that **21** is stabilized in the buffer solution. In addition, the occurrence of **15** and **9** in relatively high titers in the *A. oryzae* transformants compared to the significant lower titers of **23**, raises the question about regioselectivity and -specificity of SpoG. Due to relative instability of **21** and **23** this question cannot be answered in this context. Compound **12**, which occurred in the heterologous host (*e.g.* EXP 5), was not observed in the *in vitro* experiments, suggesting that *A. oryzae* can catalyse this transformation.

As previous reports demonstrated that lactonization can be pH-dependent,[25] *in vitro* generated **22** was acidified to pH 2 leading to partial conversion of **22** into **12** and minor quantities of **14** after 2 h of incubation (Fig. 8A). In addition to **12** and **14**, very small amounts of **13** (derived from **1**) could be found as well after increased incubation periods (Fig. 8B). This shows that lactone ring formation during sporothriolide biosynthesis can also occur spontaneously under acidic conditions, but is not enough to generate **1** in significant titers, indicating that further enzymes are required to form **1** in the natural producer.

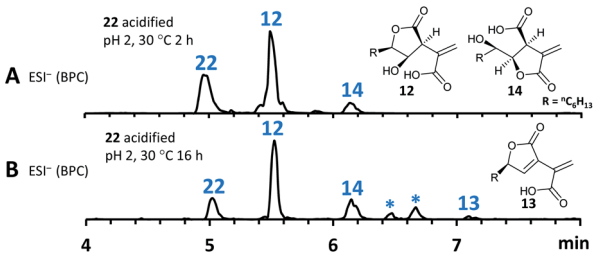

Fig. 8 Lactonization under acidic conditions. (A), ESI$^-$ spectrum of **22** (obtained directly *via* incubation of **20** with SpoG) acidified with formic acid to pH 2, at 30 °C for 2 h; (B), as (A), 30 °C for 16 h. *Unknown degradation compounds. R = ^{n}C$_6$H$_{13}$.

It is thought that ionised carboxylates which occur at higher pH values become less reactive due to being poor electrophiles,[25] therefore explaining the observed *in vitro* results. As a side note, spontaneous lactonization between C-6 hydroxy functionality and the carboxyl group of the fatty acid derived chain seems to be favoured in this case.

The cofactor dependence of SpoG was also investigated showing that α-ketoglutarate is essential for turnover *in vitro*. Furthermore, monocarboxylic acid substrates such as *trans*-2-hexenoic acid and 2-methylhexanoic acid were tested with SpoG, but did not result in observable product formation (see ESI Fig. S1.20–S1.22†).

As previously indicated the heterologous expression of the full set of genes from the *spo* cluster led to the formation of high titers of **13**, the supposed degradation product of **1**. Thus, it seems likely that the final pathway steps are catalysed by one or both encoded lactonases (SpoH, SpoJ). Attempts to express SpoH and SpoJ and study them *in vitro* in analogy to SpoG were not successful, leading to insoluble and inactive proteins in *E. coli* and non-viable colonies in *S. cerevisiae*. Further experiments therefore involved heterologous expression in *A. oryzae*.

The genes *spoH* and *spoJ* were expressed together and individually with the remaining set of genes (Table 1, EXP 6–8). Individual expression of the lactonase genes showed **12** as predominant pathway product in both cases, whereas **1** or **13** could not be detected (Fig. 6C and D). Only when both lactonases were expressed together was the final pathway product **1** observed, which quickly converted into **13** when exposed to longer fermentation periods. In addition, small titers of **14** were observed at early fermentation time points, which disappeared at the end of the fermentation period, indicating that **14** may also be a pathway intermediate that is converted into **1**.

Based on these studies a scheme for the biosynthesis of **1** can be proposed (Scheme 1). SpofasA, SpofasB, SpoE, SpoK and SpoL form octyl itaconic acid **20** as the first stable intermediate, which is converted by the dioxygenase SpoG into the C-5/C-6 hydroxylated product **22** *via* the C-5 or C-6 hydroxylated intermediates **21** and **23**. Either (or both) of **12** and **14** could be intermediates during the conversion of **22** to **1**. However, our *in vivo* experiments were unable to resolve this question and lack of soluble protein obviated *in vitro* experiments. We propose that the lactonases SpoH and SpoJ form a bifunctional heterodimer to lactonize **22** into the final pathway product **1** as neither appears to catalyse the formation of **1** in isolation. The overall route is remarkable for the number of potential shunt pathways, and we have detected at least 10 possibilities for shunt formation, of which 8 compounds have been fully characterized here.

As the biosynthesis of **1** can be fully explained by the activity of the investigated genes, the role of the unknown protein SpoI remained obscure. The function of *spoI* was especially intriguing as it showed high expression levels under both producing and non-producing conditions for **1** (see ESI Fig. S1.23–S1.26†). BLASTp[17] analysis of SpoI showed it is a member of the cupin-domain-containing proteins. It is 35.7% identical to VirC which is involved in the fungal trichoxide biosynthetic pathway,[26] although VirC is also of unknown function. Structural analysis using PHYRE-2 (ref. 18) also showed no relationship to known functionally-characterized enzymes.

To characterize SpoI, the gene was amplified from cDNA of *H. monticulosa* MUCL 54604, cloned into pET28a and overexpressed in *E. coli*. Purification of the protein in soluble form was achieved by FPLC. We first tested if SpoI could aid in the cycloaddition of sporothriolide **1** and trienylfuranol A **7** to afford sporochartines as we could not fully exclude the possibility of an enzyme catalysed reaction. Incubation of SpoI with **1** and **7** did not make the sporochartine adducts, but it resulted in the formation of small amounts of **12** and a new compound **24** which share the same molecular formula (HRMS *m*/*z* 255.1217 $[M - H]^-$; calc. for $C_{13}H_{19}O_5$, 255.1232). In addition, titers of **7** did not change throughout the experiment but **1** was consumed proving that **1** could be the substrate of SpoI (Fig. S1.26†).

The experiment was repeated with **1** as the sole substrate confirming that **1** is fully converted into **12** and **24** (Fig. 9). As the formation of **13** could be observed during the experiment it was not clear if **13** was used as substrate instead of **1**. To test this, **13** was incubated with SpoI which did not lead to product formation demonstrating that **1** is indeed the substrate of SpoI. Isolation of **24** by upscaling the *in vitro* reaction proved unsuccessful, thus the structure could not be elucidated by NMR. As **24** and **12** share the same molecular formula $C_{13}H_{20}O_5$, it was initially assumed the SpoI catalyses hydrolysis, which leads in the case of **12** to a ring opening of one of the lactones. However, the lack of **14**, **10** and **11** allows only one possible structure for **24**, where the exomethylene group is hydroxylated. As **24** was never observed in the wild type it is likely to be quickly degraded *in vivo*. The catalysed reaction of SpoI, may represent a resistance against the antifungal sporothriolide **1**, protecting the producer organism from its toxic product when it accumulates in the cells.

Finally, we investigated the distribution of fungal BGCs related to the *spo* pathway. Piliformic acid **2** is already known by labelling studies to be derived from acetate and an oxaloacetate derivative.[3]

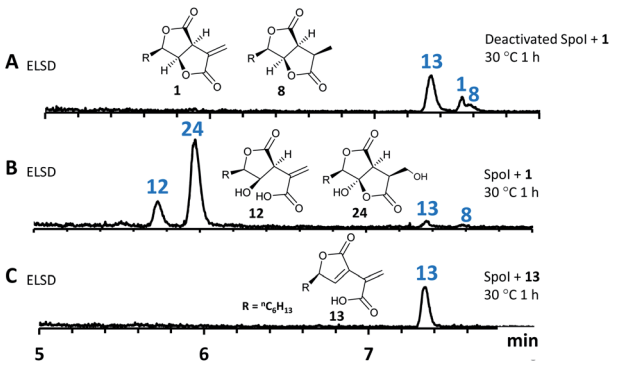

Fig. 9 *In vitro* assay of SpoI using purified proteins. (A), ELSD chromatogram of boiled SpoI (50 μM) incubated with **1** (2.5 mM) in PBS buffer (pH 7.5) at 30 °C for 1 h; (B), ELSD chromatogram of SpoI (50 μM) incubated with **1** (2.5 mM) in PBS buffer (pH 7.5) at 30 °C for 1 h; (C), ELSD chromatogram of SpoI (50 μM) incubated with **13** (2.5 mM) in PBS buffer (pH 7.5) at 30 °C for 1 h. R = $^nC_6H_{13}$.

It has been purified previously from the known producer *Xylaria hypoxylon*,[27] the genome of which we have sequenced in a parallel project.[10] Screening of the *X. hypoxylon* genome revealed a BGC with high homology to the *spo* BGC (see ESI Fig. S1.2†), but lacking *spoG*, *spoH* and *spoJ*, consistent with the lower level of oxygenation and cyclisation of **2** compared to **1**.

Multi-gene BLAST[28] analysis was performed using templates SpofasA (FAS α), SpofasB (FAS β), SpoE (citrate synthase), SpoF (transporter), SpoG (dioxygenase), SpoH (lactonase), SpoJ (lactonase), SpoK (decarboxylase) and SpoL (2-methyl citrate dehydratase) in a MultiGeneBLAST architecture search (see ESI S1.1.6 for details†). The results show that such FAS-based pathways are relatively common in fungi but have remained unrecognised to-date: modern bioinformatic tools such as antiSMASH[15] do not yet recognize such BGCs, probably because of the high number of 'primary-metabolism' related steps. At least five homologous clusters encoding fungal FAS α and β components, and citrate synthase (*spoE*), dehydratase (*spoL*), decarboxylase (*spoK*), dioxygenase (*spoG*) and one or more lactonases (*spoHJ*) were detected, predominantly in *Aspergillus* species (see ESI Fig. S1.7†), and it is likely that similar pathways will appear elsewhere.

Discussion

The sporothriolide pathway (Scheme 1) shows several points of novelty. First, a dedicated fungal FAS system produces decanoate rather than the usual octadecanoate. This differs from other known pathways such as those involved in maleidride and squalestatin biosynthesis which begin with a dedicated PKS. FAS systems which selectively form short chains should find utility in the production of biofuels, for example, where C_8 and C_{10} lipids are advantageous, and extensive efforts are underway to engineer short-chain synthases for this outcome.[29] Fungal FASs appear to have already evolved the ability to selectively produce these valuable shorter compounds, such as decanoate in **1** and octanoate in **2** and **25**, for example.

The early steps of the *spo* pathway then follow the well-known primary metabolic steps from acetyl CoA to itaconic acid, but modified to accept a longer alkyl unit. The first four steps of the pathway thus closely mirror primary metabolic steps. The presence of the decarboxylase encoded by *spoK* differentiates the pathway from those proceeding towards the maleidrides[6] where a different mode of decarboxylation appears to be coupled with multimerization catalysed by dedicated KI and PEBP enzymes,[6,30] and from the squalestatins where no dehydration or decarboxylation reactions take place, but where much more extensive backbone oxygenation leads to more complex cyclisation modes.[7]

The oxygenase SpoG catalyses the hydroxylations required to form the bis-lactone, and this moves the pathway more conclusively towards secondary metabolism. These hydroxylated intermediates are clearly able to undergo many spontaneous cyclizations, but the presence of both lactonases SpoH and SpoJ directs the pathway to sporothriolide **1**.

The presence and selectivity of the SpoG hydroxylase presumably controls the formation of related classes of metabolites in this family. For example in the case of the furofurandiones such as **1** double hydroxylation is required. Compounds such as oryzine A **25a** (Fig. 10) requires only a single hydroxylation at C-5 performed by OryG (68% identity, 77% similarity),[16] while oryzine B **25b** may arise from double hydroxylation and 3,4-dehydration. Piliformic acid **2** requires no hydroxylation. Its 2,5 unsaturation most likely arises by isomerisation of **20**, for example, consistent with the lack of a *spoG* homolog in its BGC. It also appears that the selectivity of the lactonase components (SpoHJ) may be able to control the formation of γ-lactones (*e.g.* **1**) *vs.* δ-lactones (*e.g.* **25**). Further mix-and-match experiments will be required to verify these hypotheses.[31]

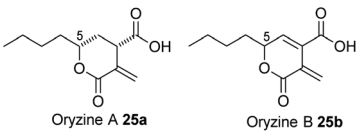

Oryzine A **25a** Oryzine B **25b**

Fig. 10 Structure of oryzines isolated from *A. oryzae*.

The identification of SpoI as a hydrolase involved in the putative self-resistance mechanism of the producer organism against **1** adds to the increasing knowledge about self-resistance genes in fungi[32] and will enable the identification of similar enzymes in other biosynthetic pathways. Knowledge of the overall pathway may also help to elucidate the BGC of more esoteric compounds such as **3** where no biosynthetic information currently exists.

Finally, we showed that, unlike in many other fungal natural products,[23,33] the DA reaction required to form the sporochartines **6a** and **6b** is spontaneous. Furthermore, no genes encoding proteins likely to be involved in the biosynthesis of trienylfuranol A **7**, such as a PKS, or other oxidative proteins, were found within or near the *spo* gene cluster. Therefore, the biosynthesis of **7** remains cryptic for now, but experiments in this area will form part of our future investigations.

Conflicts of interest

There are no conflicts to declare.

Acknowledgements

This work was supported by the Chinese Scholarship Council [Dong-Song Tian (201706670001)] and the German Research Foundation (DFG INST 187/686-1 and CO 1328/4-1). This work benefitted from the sharing of expertise within the DFG priority program "Taxon-Omics: New Approaches for Discovering and Naming Biodiversity" (SPP 1991). Prof. Marc Stadler (Helmholtz-Centre for Infection Research) and Dr Mark W Sumarah (London Research and Development Centre, Ottawa, Canada) are thanked for the gift of strains *H. monticulosa* MUCL 54604 and *H. submonticulosa* DAOMC 242471, respectively. Geraldine Le Goff is thanked for technical assistance. The bioinformatics support of the German Network for Bioinformatics Infrastructure (de.NBI) is gratefully acknowledged.

Notes and references

1 F. Surup, E. Kuhnert, E. Lehmann, S. Heitkämper, K. D. Hyde, J. Fournier and M. Stadler, *Mycology*, 2014, **5**, 110–119.
2 K. Krohn, K. Ludewig, H.-J. Aust, S. Draeger and B. Schulz, *J. Antibiot.*, 1994, **47**, 113–118.
3 N. C. J. E. Chesters and D. O'Hagan, *J. Chem. Soc., Perkin Trans. 1*, 1997, 827–834.
4 W. Weber, M. Semar, T. Anke, M. Bross and W. Steglich, *Planta Med.*, 1992, **58**, 56–59.
5 A. J. Szwalbe, K. Williams, D. E. O'Flynn, A. M. Bailey, N. P. Mulholland, J. L. Vincent, C. L. Willis, R. J. Cox and T. J. Simpson, *Chem. Commun.*, 2015, **51**, 17088–17091.
6 K. Williams, A. J. Szwalbe, N. P. Mulholland, J. L. Vincent, A. M. Bailey, C. L. Willis, T. J. Simpson and R. J. Cox, *Angew. Chem. Int. Ed.*, 2016, **55**, 6784–6788.
7 K. E. Lebe and R. J. Cox, *Chem. Sci.*, 2019, **10**, 1227–1231.
8 C. Leman-Loubière, G. Le Goff, P. Retailleau, C. Debitus and J. Ouazzani, *J. Nat. Prod.*, 2017, **80**, 2850–2854.
9 C. Leman-Loubière, G. Le Goff, C. Debitus and J. Ouazzani, *Front. Mar. Sci.*, 2017, **4**, 399.
10 D. Wibberg, M. Stadler, C. Lambert, B. Bunk, C. Spröer, C. Rückert, J. Kalinowski, R. J. Cox and E. Kuhnert, *Fungal Divers.*, 2020, DOI: 10.1007/s13225-020-00447-5.
11 L. L. Cao, Y. Y. Zhang, Y. J. Liu, T. T. Yang, J. L. Zhang, Z. G. Zhang, L. Shen, J. Y. Liu and Y. H. Ye, *Pestic. Biochem. Physiol.*, 2016, **129**, 7–13.
12 K. M. N. Burgess, A. Ibrahim, D. Sørensen and M. W. Sumarah, *J. Antibiot.*, 2017, **70**, 721–725.
13 C. Lambert, L. Wendt, A. I. Hladki, M. Stadler and E. B. Sir, *Mycol. Prog.*, 2019, **18**, 187–201.
14 C. S. Jamieson, M. Ohashi, F. Liu, Y. Tang and K. N. Houk, *Nat. Prod. Rep.*, 2019, **36**, 698–713.
15 K. Blin, S. Shaw, K. Steinke, R. Villebro, N. Ziemert, S. Y. Lee, M. H. Medema and T. Weber, *Nucleic Acids Res.*, 2019, **47**, W81–W87.
16 Z. Wasil, E. Kuhnert, T. Simpson and R. Cox, *J. Fungi*, 2018, **4**, 96.
17 M. Johnson, I. Zaretskaya, Y. Raytselis, Y. Merezhuk, S. McGinnis and T. L. Madden, *Nucleic Acids Res.*, 2008, **36**, W5–W9.
18 L. A. Kelley, S. Mezulis, C. M. Yates, M. N. Wass and M. J. E. Sternberg, *Nat. Protoc.*, 2015, **10**, 845–858.
19 F. Chen, P. Lukat, A. A. Iqbal, K. Saile, V. Kaever, J. van den Heuvel, W. Blankenfeldt, K. Büssow and F. Pessler, *Proc. Natl. Acad. Sci. U.S.A.*, 2019, **116**, 20644–20654.
20 M. L. Nielsen, L. Albertsen, G. Lettier, J. B. Nielsen and U. H. Mortensen, *Fungal Genet. Biol.*, 2006, **43**, 54–64.
21 S. Jenni, M. Leibundgut, D. Boehringer, C. Frick, B. Mikolásek and N. Ban, *Science*, 2007, **316**, 254–261.
22 L. Liu, Y. Han, J. Xiao, L. Li, L. Guo, X. Jiang, L. Kong and Y. Che, *J. Nat. Prod.*, 2016, **79**, 2616–2623.
23 L. Kahlert, E. F. Bassiony, R. J. Cox and E. J. Skellam, *Angew. Chem. Int. Ed.*, 2020, **59**(14), 5816–5822.
24 J. Qi, D. Wan, H. Ma, Y. Liu, R. Gong, X. Qu, Y. Sun, Z. Deng and W. Chen, *Cell Chem. Biol.*, 2016, **23**, 935–944.
25 Z. Zhang, P. Gibson, S. B. Clark, G. Tian, P. L. Zanonato and L. Rao, *J. Solution Chem.*, 2007, **36**, 1187–1200.
26 L. Liu, M. C. Tang and Y. Tang, *J. Am. Chem. Soc.*, 2020, **141**, 19538–19541.
27 J. R. Anderson, R. L. Edwards and A. J. S. Whalley, *J. Chem. Soc., Perkin Trans. 1*, 1985, 1481–1485.
28 M. H. Medema, E. Takano and R. Breitling, *Mol. Biol. Evol.*, 2013, **30**, 1218–1223.
29 J. Gajewski, F. Buelens, S. Serdjukow, M. Janßen, N. Cortina, H. Grubmüller and M. Grininger, *Nat. Chem. Biol.*, 2017, **13**, 363–365.
30 R. Schor and R. Cox, *Nat. Prod. Rep.*, 2018, **35**, 230–256.
31 C. Schotte, L. Li, D. Wibberg, J. Kalinowski and R. J. Cox, *Angew. Chem. Int. Ed.*, 2020, DOI: 10.1002/anie.202009914.
32 N. P. Keller, *Nat. Chem. Biol.*, 2015, **11**, 671–677.
33 R. Schor, C. Schotte, D. Wibberg, J. Kalinowski and R. J. Cox, *Nat. Commun.*, 2018, **9**, 1963.